JOC Article

Structure/Reactivity Relationships in the Benzo[*c*]phenanthrene Skeleton: Stable Ion and Electrophilic Substitution (Nitration, Bromination) Study of Substituted Analogues, Novel Carbocations and Substituted Derivatives

Cédric Brulé,[†] Kenneth K. Laali,*[,†] Takao Okazaki,[†] and Mahesh K. Lakshman[‡]

Department of Chemistry, Kent State University, Kent, Ohio 44242, and The City College and The City University of New York, 138th Street at Convent Avenue, New York, New York 10031

klaali@kent.edu

Received December 12, 2006

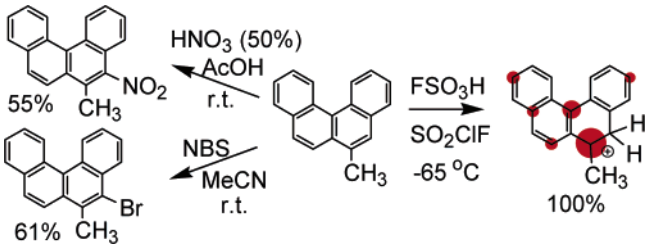

A series of novel carbocations were generated by low-temperature protonation of substituted benzo[*c*]-phenanthrenes, B[*c*]Phs, and their charge delocalization pathways were elucidated by NMR on the basis of the magnitude of $\Delta\delta^{13}$C values. It has been shown that the protonation regioselectivity is strongly controlled by methoxy and hydroxyl substituents, whose directive effects override methyl substitution effects. Regiocontrol by −OMe and −OH substituents, and its stronger influence relative to methyl groups, was also observed in the nitration and bromination reactions. Charge distribution modes in the regioisomeric protonated carbocations formed via parent B[*c*]Ph as well as in the benzylic carbocation formed via fjord-region epoxide ring opening were deduced by gauge-invariant atomic orbital density functional theory (GIAO-DFT) and from the natural population analysis (NPA)-derived changes in charges over CHs. These patterns were compared with those derived from NMR experiments in the substituted derivatives. NMR-based charge delocalization mapping provided insight into structure/activity relationships in the methylated and fluorinated B[*c*]Phs. Regioselectivities observed in the nitration and bromination reactions in representative cases are the same as those via protonations. Among a group of novel nitro and bromo derivatives synthesized in this study are examples, where the nitro group is introduced into the fjord region, for which the X-ray structure could be obtained in one case.

Introduction

Parent benzo[*c*]phenanthrene (B[*c*]Ph) **1** is the smallest polycyclic aromatic hydrocarbon (PAH) with a fjord region (Figure 1). As the first member of the [*n*]-helicenes family,[1] **1** has a twisted framework with an angle of 27° between the A and D rings from the X-ray structure.[2]

B[*c*]Ph is produced in the environment by incomplete combustion and has been identified in food, cigarette smoke, and wastewater.[3a] Parent **1** is weakly carcinogenic in animal tests, in which B[*c*]Ph-5,6-dihydrodiol is produced as the major oxidized product and B[*c*]Ph-3,4-dihydrodiol formation is minor.[3a] Interestingly, the opposite regioselectivity is exhibited in human metabolism, whereby B[*c*]Ph-3,4-dihydrodiol (a

* Corresponding author. Fax: 330-672-3816. Tel: 330-672-2988.
[†] Kent State University.
[‡] The City College and The City University of New York.

(1) (a) Portella, G.; Poater, J.; Bofill, J. M.; Alemany, P.; Solà, M. *J. Org. Chem.* **2005**, *70*, 2509. (b) Hopf, H. *Classics in Hydrocarbon Chemistry*; Wiley-VCH: Weinheim, 2000; Chapter 12.

(2) (a) Lakshman, M. K.; Kole, P. L.; Chaturvedi, S.; Saugier, J. H.; Yeh, H. J. C.; Glusker, J. P.; Carrell, H. L.; Katz, A. K.; Afshar, C. E.; Dashwood, W. M.; Kenniston, G.; Baird, W. M. *J. Am. Chem. Soc.* **2000**, *122*, 12629. (b) Hirshfeld, F. L.; Sandler, S.; Schmidt, G. M. J. *J. Chem. Soc.* **1963**, 2108.

10.1021/jo0625453 CCC: $37.00
Published on Web 03/30/2007

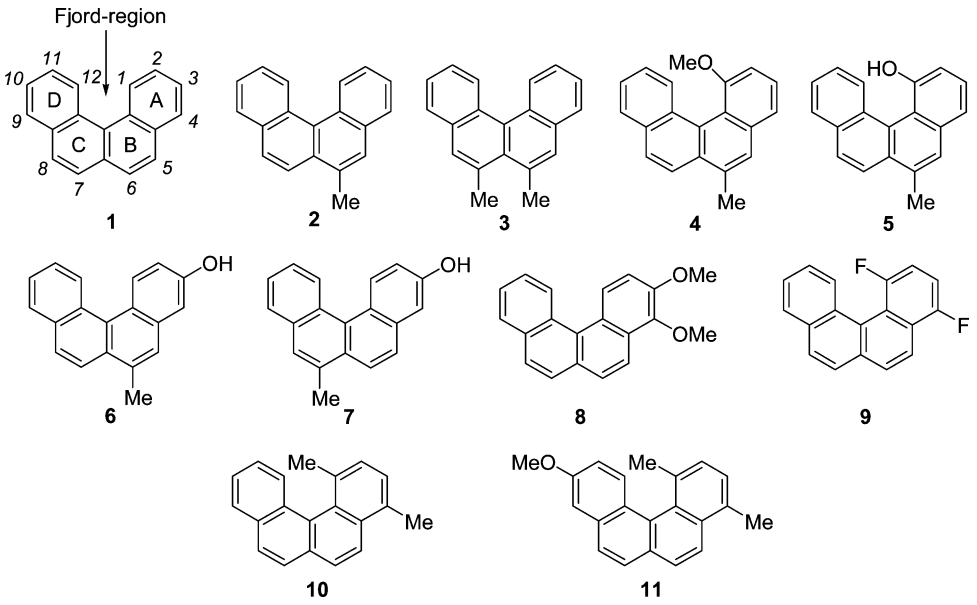

FIGURE 1. Substituted benzo[*c*]phenanthrenes studied.

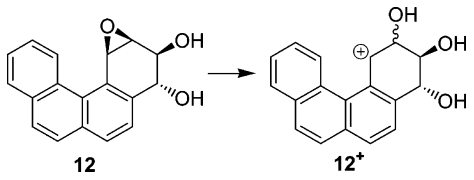

FIGURE 2. Benzylic carbocation formation in metabolic activation of B[*c*]Ph.

proximate carcinogen) is the main product (B[*c*]Ph-3,4-dihydrodiol is the minor pathway), which is further oxidized to B[*c*]-Ph-3,4-diol-1,2-epoxides (ultimate carcinogens), with the (−)-*anti*-diol epoxide being more potent.[3a] Dipple and associates[3b] reported that B[*c*]Ph-3,4-diol-1,2-epoxides are exceptionally good DNA alkylating agents, with each configurational isomer exhibiting marked preference for covalent binding to DNA over hydrolysis and each reacting extensively with deoxyadenosine. Metabolic studies by Baird and co-workers[3c] and by Eisenbrand and associates[3a] demonstrated that B[*c*]Ph-3,4-diol-1,2-epoxides are formed from B[*c*]Ph in the human mammary carcinoma cell line (MCF-7) and via oxidative metabolism in the human liver and lung. The results underscored that B[*c*]Ph is potentially more toxic in humans than in rodents.

Despite its remarkably high tumorigenicity, the solvolytic reactivity (in both acid-catalyzed and neutral hydrolysis) of the *anti*-diol epoxide of B[*c*]Ph was reported to be relatively low,[3d] and it is plausible that the observed high levels of DNA alkylation could stem from the longer lifetime of the metabolites.

Given the significance of the fjord-region epoxide of B[*c*]Ph in human metabolism, studies focusing directly on the benzylic carbocation (**12** → **12**$^+$) (Figure 2) are quite relevant.

Focusing on structure/activity relationships, the 3-, 4-, 5-, and 6-methylated derivatives of B[*c*]Ph were found to be tumorigenic in mouse skin, but the 1-Me and 2-Me derivatives were less active than the parent B[*c*]Ph.[4] Fluorine substitution on the benzo ring enhanced tumorigenicity relative to parent **1**, except for the 2-fluoro derivative which was less active.[5a] Fluorine substitution at C-6 increased tumorigenic activity by over 4-fold.[5b]

Nitration, acetylation, and bromination of parent **1** were studied by Newman and Kosak in the 1940s, showing preferential substitution at C-5.[6]

Methyl substitution into the highly congested fjord region increases skeletal distortion from 27° for the A/D ring angle in B[*c*]Ph to 37° for that in 1,4-dimethyl-B[*c*]Ph (compound **10** in Figure 1).[2] Increased nonplanarity in **10** lowers its metabolic activation, relative to parent B[*c*]Ph, to form DNA alkylating species with MCF-7 cells.[2] More recently, the 1,4-difluoro-B[*c*]-Ph **9** and its dihydrodiol have been synthesized.[7] The A/D angle in **9** is about 33°, but the dihydrodiol is less twisted (A/D angle 22°). There are some notable features in the dihydrodiol and diol epoxide derivatives of B[*c*]Ph **1**, **9**, and **10**. Whereas in each case the dihydrodiols exhibit a quasi-diequatorial arrangement of the hydroxyl groups, conformational preference in the diol epoxides of **1** and **9** are different. For **1**, both *syn*- and *anti*-diol epoxides exhibit a predominantly quasi-diequatorial arrangement of the hydroxyls, but for **9**, the OH groups are quasi-diaxial in the *syn*-diol epoxide and quasi-diequatorial in the *anti*-diol epoxide.[5a,7]

(3) (a) Baum, M.; Amin, S.; Guengerich, F. P.; Hecht, S. S.; Köhl, W.; Eisenbrand, G. *Chem. Res. Toxicol.* **2001**, *14*, 686. (b) Dipple, A.; Pigott, M. A.; Agrawal, S. K.; Yagi, H.; Sayer, J. M.; Jerina, D. M. *Nature* **1987**, *327* (6122), 535. (c) Einolf, H. J.; Amin, S.; Yagi, H.; Jerina, D. M.; Baird, W. M. *Carcinogenesis* **1996**, *17*, 2237. (d) Sayer, J. M.; Yagi, H.; Croisy-Delcey, M.; Jerina, D. M. *J. Am. Chem. Soc.* **1981**, *103*, 4970.

(4) Hecht, S. S.; Melikian, A. A.; Amin, S. In *Polycyclic Aromatic Hydrocarbon Carcinogenesis: Structure−Activity Relationships*; Yang, S.K., Silverman, B.D., Eds.; CRC press: Boca Raton, FL, 1988; Vol.1, Chapter 4.

(5) (a) Jerina, D. M.; Sayer, J. M.; Yagi, H.; Croisy-Delcey, M.; Ittah, Y.; Thakker, D. R.; Wood, A. W.; Chang, R. L.; Levin, W.; Conney, A. H. In *Biological Reactive Intermediates II*, Part A; Snyder, R., Parke, D. V., Kocsis, J. J., Jollow, D. J., Gibson, C. G., Witmer, C. M., Eds.; Plenum Press: New York, 1982; pp 501−523. (b) Mirsadeghi, S.; Prasad, G. K. B.; Whittaker, N.; Thakker, D. R. *J. Org. Chem.* **1989**, *54*, 3091.

(6) Newman, M. S.; Kosak, A. I. *J. Org. Chem.* **1949**, *14*, 375.

(7) Bae, S.; Mah, H.; Chaturvedi, S.; Musafia, T. J.; Baird, W.; Katz, A. K.; Carrell, H. L.; Glusker, J. P.; Okazaki, T.; Laali, K. K.; Zajc, B.; Lakshman, M. K., to be published.

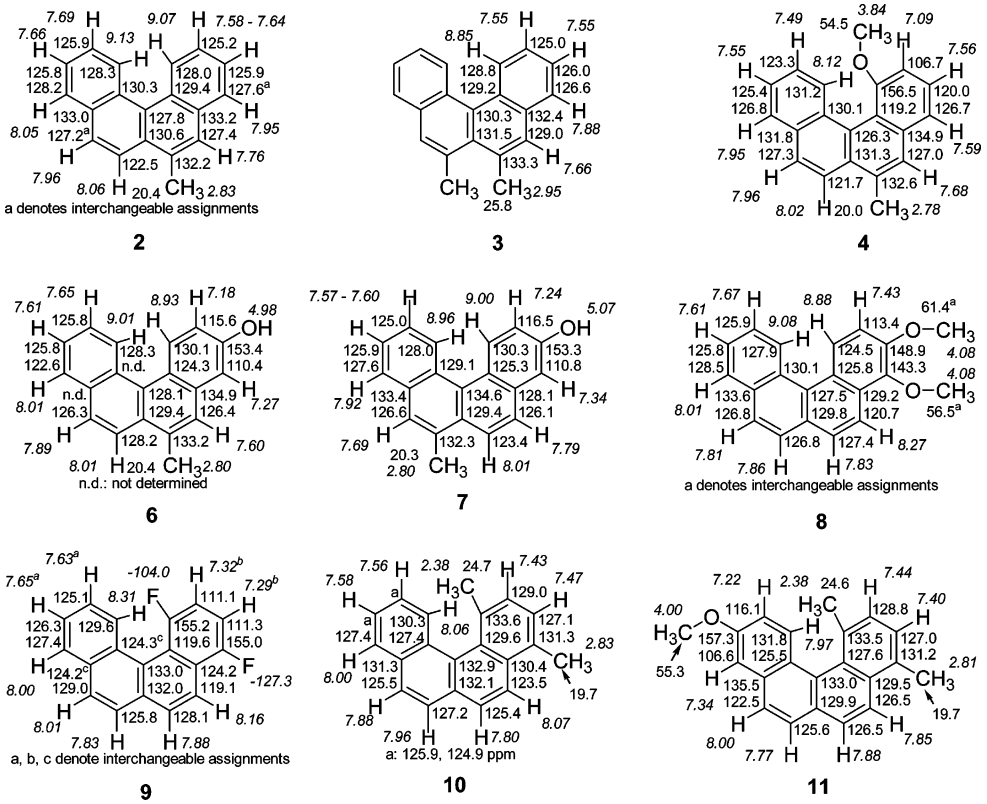

FIGURE 3. Specific ^{1}H (italic) and ^{13}C NMR assignments for the B[*c*]Ph derivatives.

As part of a broader stable ion and electrophilic substitution study,[8] we showed that nitration and benzoylation of parent **1** gave the corresponding 5-substituted derivatives, and a methoxy or a hydroxyl substituent at C-3 directed the electrophilic attack to C-4 (in stable ion protonation and/or protic nitration).

In an effort to gain more insight into structure/reactivity relationships in the B[*c*]Ph skeleton, the present study focuses on stable ion and electrophilic chemistry of a relatively large group of substituted derivatives, including those with substituents in the fjord region (see Figure 1).

Results and Discussion

NMR of Neutral PAHs. Complete NMR assignments were made with the aid of 2D NMR and NOE for the B[*c*]Ph derivatives listed in Figure 1 (except for compound **5**; see later), and the data are gathered in Figure 3. The following general features are noteworthy. The fjord-region protons (H-1 and H-12) are highly deshielded (appear around 9 ppm). The presence of a substituent at position 1 shields the H-12 by about 1 ppm. In the 1,4-difluoro-substituted derivative (**9**), the fjord-region fluorine is deshielded by 23 ppm relative to the other fluorine.

Generation and Direct NMR Study of the Carbocations (Schemes 1−3, Figures 4 and 5). Low-temperature protonation of the 6-Me derivative **2** (Scheme 1) with FSO_3H in SO_2ClF at −65 °C led to the formation of $\mathbf{2H}^+$ (protonation at C-5) as the only detectable carbocation. The most deshielded carbon resonances in $\mathbf{2H}^+$ are due to C-6 (δ 203.8) and C-12b (δ 160.3) (Figure 4), with extensive charge delocalization into rings B and C (Figure 5).

SCHEME 1. Protonation of 2−4 in FSO_3H/SO_2ClF

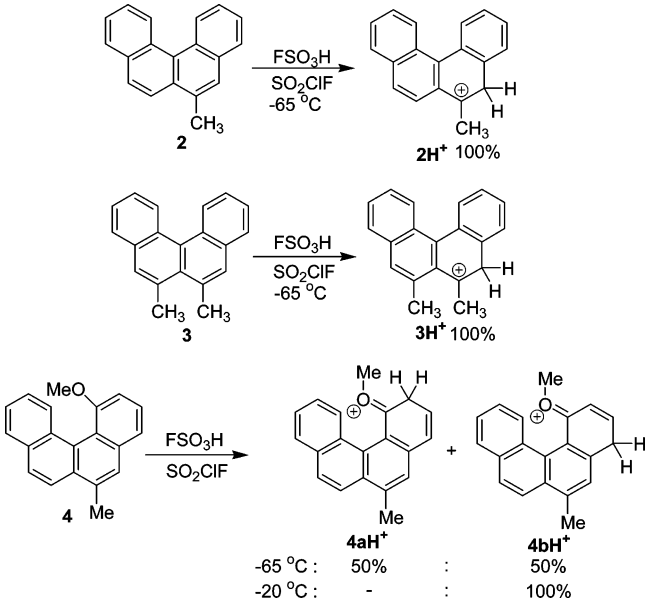

Introduction of a second methyl substituent at C-7 (compound **3**) did not change the protonation regioselectivity, generating carbocation $\mathbf{3H}^+$ (attack at C-5), leading to loss of symmetry (Scheme 1). Despite the presence of two methyl groups, the positive charge remains strongly localized on C-6 (δ 197.0). It is interesting to note that the fjord-region protons in both **2** and **3** (Figure 3) are more deshielded than those in the corresponding carbocations $\mathbf{2H}^+$ and $\mathbf{3H}^+$ (Figure 4), reflecting conformational change as a way to lower steric strain.

Compound **4** with a methoxy group in the fjord region and a methyl group at C-6 provided the opportunity to explore

(8) Laali, K. K.; Okazaki, T.; Kumar, S.; Galembeck, S. E. *J. Org. Chem.* **2001**, *66*, 780.

SCHEME 2. Protonation of Compounds 5−7

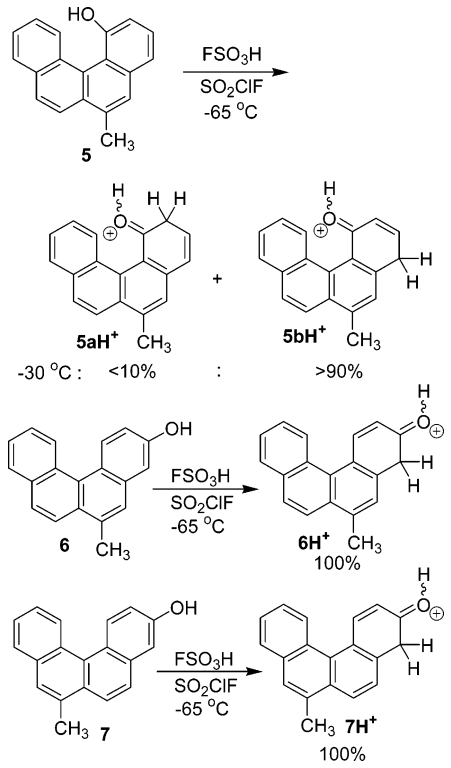

relative effectiveness of these groups in directing electrophilic attack. Protonation of **4** with FSO_3H/SO_2ClF at −65 °C (Scheme 1) yielded a 1:1 mixture of the two regioisomers **4aH**$^+$ and **4bH**$^+$ (protonation ortho/para to methoxy). Warming the mixture to −20 °C during 15−20 min resulted in complete isomerization of **4aH**$^+$ to **4bH**$^+$, thus establishing **4aH**$^+$ as the kinetic and **4bH**$^+$ as the thermodynamic carbocation. This isomerization is irreversible, thus allowing complete NMR characterization of **4bH**$^+$ alone to be made at −50 °C. Specific proton NMR assignments for each regioisomer were made via NOE enhancements.

The methylene protons are diastereotopic in both **4aH**$^+$ and **4bH**$^+$ giving rise to doublets with 27−30 Hz coupling, corresponding to a *gem* relationship. Whereas in **4bH**$^+$ the ^{1}H NMR chemical shift values for the two geminal protons are quite close (Δppm = 0.08), this difference is larger in the case of **4aH**$^+$ (Δppm = 0.30). The methoxy group in **4aH**$^+$ is in a sterically congested environment due to both the fjord region and the *ortho*-methylene group and is forced to adopt an out-of-plane conformation for the O−CH_3 bond. Consequently, the two protons of the methylene group in **4aH**$^+$ appear in different environments, with a larger difference in chemical shifts. The positive charge in both **4aH**$^+$ and **4bH**$^+$ is delocalized within a naphthalenium moiety plus one conjugated carbon (Figure 5).

The outcome of low-temperature protonation of compound **5** (this compound was available in a very small quantity) was similar to **4**, leading to a mixture of two regioisomers **5aH**$^+$ and **5bH**$^+$ (Scheme 2). However, in this case, the proton resonances were broad, and this prevented specific assignments. As with **4**, isomerization of **5aH**$^+$ into **5bH**$^+$ was observed upon raising the temperature to −30 °C for 20 min. Only partial NMR assignments for **5bH**$^+$ could be achieved at −40 °C (Figure 4). Skeletally intact **5** was recovered upon quenching, and the substrate was used for bromination (see later).

Low-temperature reaction of compound **6** with FSO_3H/SO_2ClF at −65 °C (Scheme 2) resulted in quantitative formation of carbocation **6H**$^+$ (protonation at C-4), demonstrating that an OH group in the A-ring is much more effective in directing electrophilic attack compared to a methyl group in the K-region. The positive charge in **6H**$^+$ is heavily localized in the A-ring plus a conjugated carbon in the B-ring (Figure 5). The fjord-region protons in **6H**$^+$ have very different chemical shifts (with H-1 at 9.74 ppm and H-12 at 8.33 ppm).

A similar directive effect is exhibited in the low-temperature protonation of **7** (Scheme 2), which led to quantitative formation of **7H**$^+$ (protonation at C-4). The NMR characteristics and charge delocalization modes in **6H**$^+$ and **7H**$^+$ are very similar. Thus, methyl substitution in the K-region has no control over the protonation outcome, when an OH group is present in the A-ring.

Low-temperature protonation of the 3,4-dimethoxy derivative **8** under the same set of conditions resulted in a complex mixture that could not be specifically analyzed. Similarly, the low-temperature reaction of the 1,4-difluoro derivative **9** gave a complex spectrum with indication for gradual decomposition. Nevertheless, skeletally intact **9** could be recovered in relatively good yield upon quenching of the superacid solution.

Initial NMR spectra recorded immediately after reacting 1,4-DMB[*c*]Ph **10** with FSO_3H/SO_2ClF at −65 °C showed evidence for C-protonation due to the presence of a methylene group appearing as a pair of doublets with geminal coupling. However, minutes later, broad signals appeared and the spectral resolution greatly diminished. These features suggested competing oxidation with the formation of a radical cation, rather than side reactions, because the starting material **10** was recovered intact upon quenching (together with a small amount of side products).

Interestingly, introduction of a methoxy group into the other outer ring of **10** produced a different protonation outcome. Thus, the low-temperature reaction of **11** with FSO_3H/SO_2ClF at −65 °C (Scheme 3) gave a 4:1 mixture of **11aH**$^+$ and **11bH**$^+$ as distinct conformers, with protonation directed ortho to methoxy (at C-9). On the basis of NOE studies, the major conformer **11aH**$^+$ corresponds to a less-hindered conformation with OMe pointing toward H-11, whereas the minor conformer **11bH**$^+$ corresponds to the conformation with OMe facing CH_2. On raising the temperature to −30 °C, these merged into a single averaged species **11H**$^+$. The charge delocalization mode in **11H**$^+$, as well as in **11aH**$^+$ and **11bH**$^+$, is analogous to those of **6H**$^+$ and **7H**$^+$. The protonation outcome underscores the directive effect of the methoxy group in **11**.

Computational Study

As reported previously, attempts to generate a stable carbocation from parent **1** were unsuccessful. However, protic nitration (HNO_3/HOAc) and benzoylation ($PhCOCl/AlCl_3$) as prototypic electrophilic substitution reactions resulted in C-5 substituted derivatives.[8] According to DFT calculations by B3LYP/6-31G(d),[9] the arenium ion of protonation of B[*c*]Ph at C-5 is more stable than those derived from protonation at C-1, C-4, C-6, C-2, and C-3 by 2.7, 2.7, 3.4, 3.5, and 3.7 kcal/mol, respectively (Table S1 in Supporting Information.)

The charge delocalization modes in benzo[*c*]phenanthrenium cations **1aH**$^+$ (C-2 protonated), **1bH**$^+$ (C-4 protonated), and **1cH**$^+$ (C-5 protonated), which are not accessible via experimental stable

(9) Koch, W.; Holthausen, M. C. *A Chemist's Guide to Density Functional Theory*, 2nd ed.; Wiley-VCH: Weinheim, 2000.

SCHEME 3. Protonation of 11

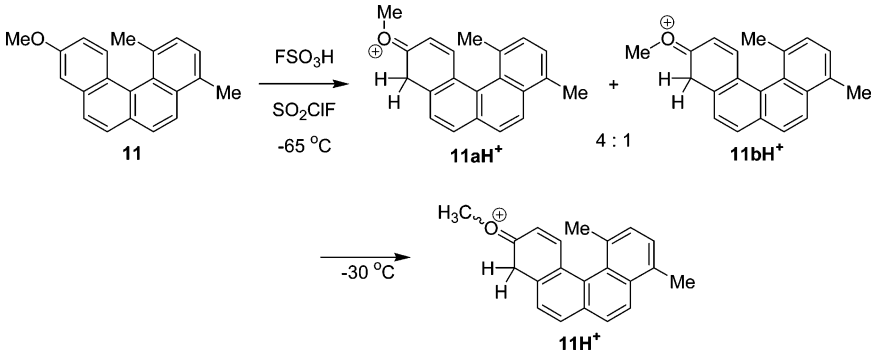

ion studies, were derived on the basis of the magnitude of $\Delta\delta^{13}$C values, computed by gauge-invariant atomic orbital density functional theory (GIAO-DFT),[9] for comparison with the NMR-derived values summarized in Figure 5. In addition, the charge delocalization mode for the benzylic carbocations formed via fjord-region epoxide ring opening (**13a**$^+$) was also calculated for comparison (see Figure 6).

To examine the charge pattern by another approach, the natural population analysis (NPA)-derived changes in charges over CHs were computed by DFT for **12a**$^+$/**12b**$^+$ and **13a**$^+$/**13b**$^+$ (see Figure 7).

NPA-derived changes in charges in benzylic carbocations formed by epoxide ring opening indicate no significant positive charge retention at the benzylic carbocation center and charge accumulation at C-3, C-4a, C-6, C-10, and C-12b, with C-6 exhibiting the largest positive localization. Introduction of carbocation-stabilizing substituents (methyl and fluorine) at C-3/C-6/C-10 will stabilize the carbocation, and this concurs with the observed increased bioactivity in the 6-Me, 3-Me, and 6-F derivatives but does not provide a basis for understanding the increased activity in the 4-Me and 5-Me derivatives. To test the effect of fluorine/methyl substitution, the NPA-derived changes of charges in the fluorinated carbocations **14**$^+$, **15**$^+$, and **16**$^+$ (Figure 8) and the carbocations **17**$^+$, **18**$^+$, and **19**$^+$ (Figure 9) were computed. These substitutions did not cause notable changes in the charge delocalization mode (the positive charge is still primarily delocalized into C-3, C-4a, C-6, C-10, and C-12b). In **19**$^+$, in addition to the indicated ring positions, the methyl group also becomes notably positive.

Comparing the GIAO-derived $\Delta\delta^{13}$C patterns (Figure 6) with experimental $\Delta\delta^{13}$C values (Figure 5) and the NPA-derived charge maps (Figure 7), it can be seen that **1aH**$^+$ and **13**$^+$ are analogous to **4aH**$^+$, that **1bH**$^+$ is similar to **4bH**$^+$, **6H**$^+$, **7H**$^+$, and **11H**$^+$, and that **1cH**$^+$ is similar to **2H**$^+$ and **3H**$^+$. Therefore, the arenium ions can be viewed as rational models for studying substituent effects and charge delocalization modes via the epoxides.

Probing Substituent Effects Through Electrophilic Substitution Reactions. Nitration and bromination were used as prototypic reactions to examine substituent effects in the B[*c*]Ph derivatives, with the aim to compare the resulting regioselectivities with the protonation outcomes. The results of these reactions are summarized in Schemes 4 and 5.

Two sets of conditions were typically employed in protic nitration, namely, HNO_3 (50% aqueous)/AcOH at room temperature (method A) and HNO_3 alone (20% aqueous) at low temperature (method B).[10] The milder conditions were used in the nitration of the methoxy derivatives. For bromination reactions, a modified procedure reported by Mitchell et al. was used (method C).[11] Limited availability of the PAHs was the determining factor in the number of derivatives that could be synthesized.

Nitration of **2** using method A yielded **2NO$_2$** (substitution at C-5) in 55% isolated yield. The starting material was totally consumed, and some side products were also present (probably corresponding to various isomeric dinitrated compounds). Mild bromination of **2** gave the 5-bromo derivative **2Br** in 61% yield. It follows that the regioselectivity in nitration and bromination of **2** is the same (substitution at C-5) as that observed in the stable ion study.

Bromination of **4** (OMe group in the fjord region) yielded **4Br** in 88% yield by substitution at C-4 (para to methoxy), whereas, as described earlier, protonation of **4** yielded both **4aH**$^+$ (ortho) and **4bH**$^+$ (para) carbocations. Absence of a C-2 brominated product reflects the higher energy of its arenium ion due to steric crowding.

Bromination of **5** (OH group in the fjord region) yielded the monobromo derivative **5aBr** (substitution at C-4; para to OH) in 48% isolated yield and an equimolar mixture of **5bBr** (substitution at C-2; ortho to OH) and the 2,4-dibromo derivative **5cBr**. The latter two compounds (combined yield 43%) could not be separated by preparative TLC, but their constitution was confirmed by electrospray mass spectrometry. Formation of **5cBr** was likely due to the use of a small excess of NBS (1.3 equiv).

By employing method A in the nitration of the dimethoxy derivative **8**, the dinitro- and trinitro-substituted derivatives **8bNO$_2$** and **8cNO$_2$** were obtained (in 25% and 27% yields, respectively), together with other unidentified products (likely polynitrated compounds that could not be isolated). However, mild nitration of **8** (using method B) gave the novel mononitrated product **8aNO$_2$** by nitration in the fjord region in 94% isolated yield. Recrystallization of **8aNO$_2$** produced yellow crystals suitable for X-ray analysis (Figure 10). It is noteworthy that the presence of the nitro group in the fjord region increases the helicity of the system relative to parent B[*c*]Ph so that the torsion angle between the rings A and D increases from 26.7°[2] to 29.3°. The average dihedral angle formed between the nitro group and the aromatic plane of the A-ring is 28.3°. Relative to the A-ring, the nitro group is severely buttressed with an out-of-plane angle of 16.2°.

Attempted selective protic nitration of 1,4-DFB[*c*]Ph **9** was unsuccessful under a variety of conditions. Nitration of **9** with a stoichiometric amount of the nitronium tetrafluoroborate (NO_2BF_4) in CH_3CN at room temperature overnight led to a mixture of two mononitro isomers (total 24%), with 36% of **9** remaining unreacted (corresponding to 64% of the total conversion). Formation of the isomeric mononitro derivatives was corroborated by ES-MS and by ^{19}F NMR (see Experimental Section). Regioselectivity in nitration could not be established via NOE due to the close proximity of the aromatic ^{1}H NMR signals. Attempted bromination of **9** with NBS/CH_3CN gave no conversion even at reflux in CH_3CN!

Nitration of 1,4-DMB[*c*]Ph **10** was attempted under various conditions. However, in all cases, the starting material underwent degradation. Therefore, no nitro derivative of **10** could be synthesized via conventional means. Attempted bromination of **10** (NBS/CH_3CN) led to low conversion (even after 2 days at reflux). Among

(10) Ferlin, M. G.; Chiarelotto, G.; Malesani, G. *J. Heterocycl. Chem.* **1989**, *26*, 245.
(11) Mitchell, R. H.; Lai, Y.-H.; Williams, R. V. *J. Org. Chem.* **1979**, *44*, 4733.

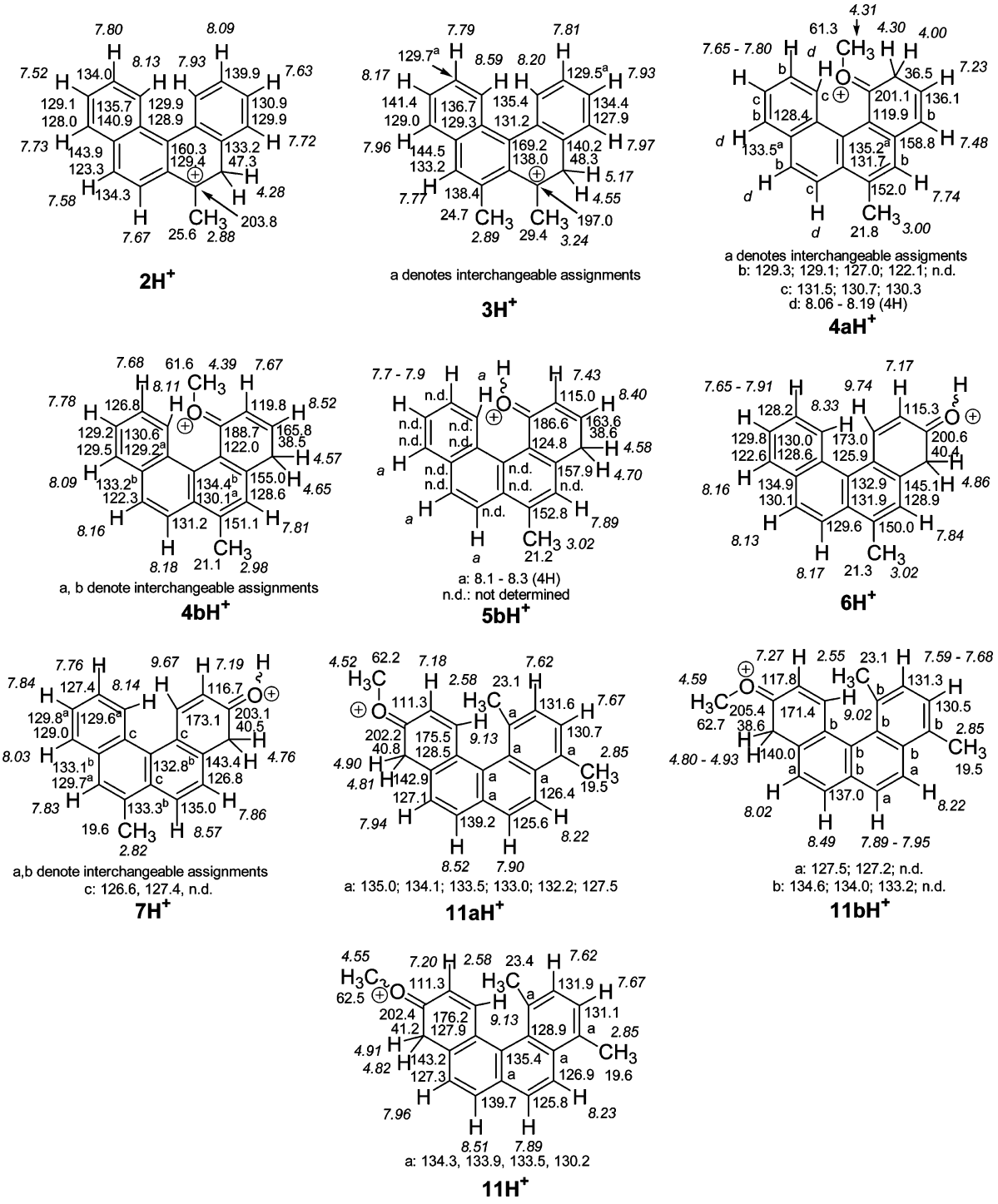

FIGURE 4. ^{1}H (italic) and ^{13}C NMR data for the carbocations.

the formed products, a monobrominated compound was detected by TLC and by ES-MS.

Contrary to the unexpected reactivity pattern in **10**, the methoxy-substituted analogue **11** was successfully nitrated by using 30% HNO_3 at −10 °C, yielding a 3:2 mixture of regioisomeric mononitrated derivatives **11aNO$_2$** and **11bNO$_2$**, respectively (in 53% yield). Because the isomeric mixture could not be separated by preparative TLC, they were analyzed as a mixture by ^{1}H NMR and ES-MS. The position of the nitro group could only be determined unambiguously in the case of **11aNO$_2$** via NOE experiments. Bromination of **11** resulted in the isolation of **11Br** in quantitative yield (bromine at C-9). Overall, electrophilic reactivity studies on **11** establish a common pattern in protonation, nitration, and bromination, showing that the regioselectivity is controlled by the methoxy group, leading in all cases to substitution at C-9.

Comparative Discussion and Summary

Protonation, nitration, and bromination data for the K-region monomethylated compound **2** and protonation data for the dimethyl derivative **3** indicate that in all cases electrophilic addition is directed to C-5. However, the K-region methyl groups are no longer in control of regioselectivity, once methoxy

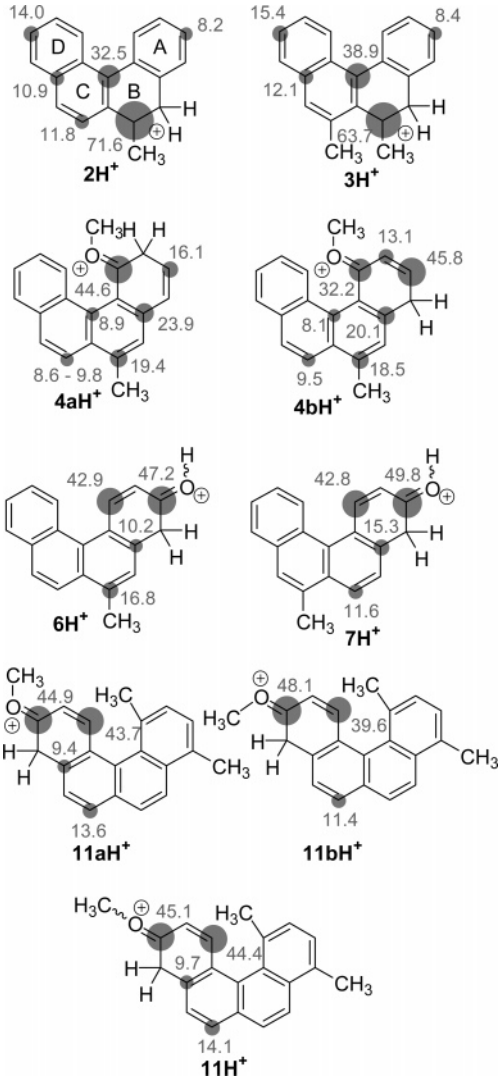

FIGURE 5. Charge delocalization modes derived from experimental $\Delta\delta^{13}$C values (carbocation minus neutral) (threshold 8 ppm).

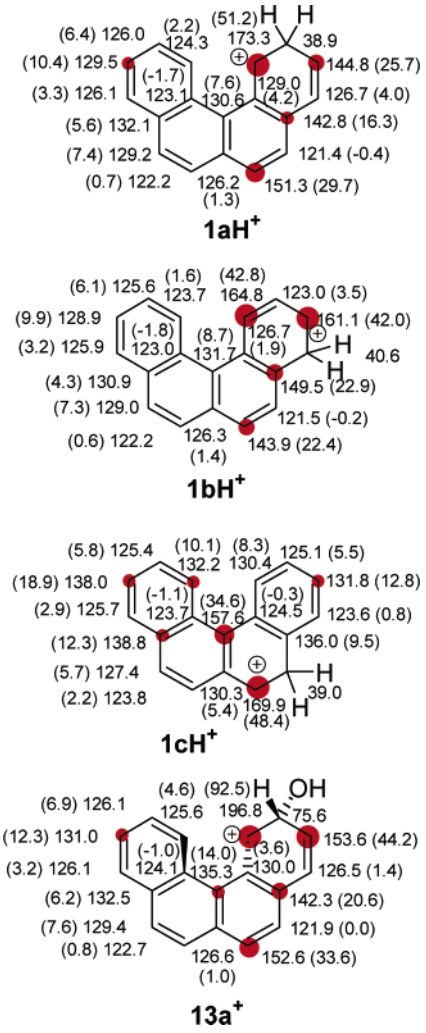

FIGURE 6. GIAO-NMR chemical shifts for model benzo[*c*]phenanthrenium ions **1aH**$^+$, **1bH**$^+$, **1cH**$^+$, and **13a**$^+$ and $\Delta\delta^{13}$C values (in parentheses) relative to computed GIAO data for parent B[*c*]Ph or 2-hydroxy-B[*c*]Ph (dark circles signify the sites with notable $\Delta\delta^{13}$C values).

or hydroxyl groups are introduced into the outer ring. This is seen in protonation and bromination of **4**, in bromination and protonation of **5**, in protonation of **6** and **7**, in nitration of **8**, and in protonation, nitration, and bromination of **11**. In such cases, initial electrophilic attack is directed to the outer ring, ortho/para to OH or OMe substituents.

The charge delocalization pattern established in the resulting carbocation intermediates based on $\Delta\delta^{13}$C values (Figure 5) is analogous to that derived from GIAO-DFT for the benzylic carbocation formed via fjord-region epoxide ring opening.[8] Positive charges in the substituted 5-benzo[*c*]phenanthrenium ions are delocalized extensively into the B and C rings and charges in the 2- or 4-benzo[*c*]phenanthrenium ion derivatives are delocalized into the A rings and conjugated carbons in the B rings. All carbocations have significant charge localization at the C-3 and C-6 positions. It is, therefore, reasonable to consider these model carbocations and their charge delocalization maps as a basis for predicting substituent effects, for comparison with the available biological data. This approach rationalizes the increased activity of the 3-Me, 6-Me, and 6-F derivatives, as these strategic substitutions stabilize the benzylic carbocation intermediate. Methyl substitution at C-2 creates steric hindrance to bay-region epoxidation and inhibits tumorigenic activity, despite the fact that epoxidation could still occur in the other benzo ring. Similarly, fluorine substitution at C-2 has been shown to decrease tumorigenic activity, even though in principle epoxidation could still occur in the other benzo ring. The DFT study infers that if this could occur charge delocalization in the resulting carbocation is not influenced by the presence of fluorine at C-11. Further studies (synthesis of DNA adducts and computational modeling) are warranted to help rationalize these points.

The greatly increased tumor-initiating activities of the 6-Me and the 6-F derivatives are clear indications for the importance of fjord-region diol epoxides, because these substituents can inhibit metabolism at the K-region. The present study underscores the higher stability of the benzylic carbocation, when carbocation stabilizing groups are present at C-6 and C-3. Obviously, the bigger picture needs to take into account steric and planarity factors, in particular, in the case of **9**−**11** because it was shown previously that **10** produces only low levels of DNA adducts in MCF-7 cells.[2a]

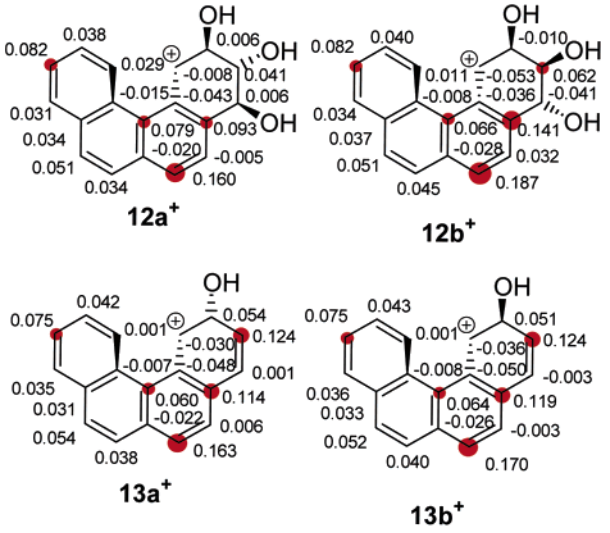

FIGURE 7. NPA-derived changes in charges over CHs relative to neutral precursors (dark circles are roughly proportional to the magnitude of changes; threshold = 0.06).

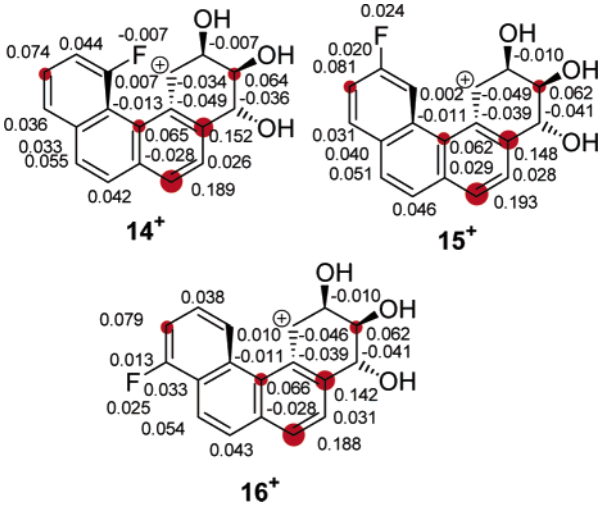

FIGURE 8. NPA-derived changes in charges over CHs relative to neutral precursors (dark circles are roughly proportional to the magnitude of changes; threshold = 0.06).

Finally, the present study has resulted in the synthesis, isolation, and characterization of a host of nitro- and bromo-substituted derivatives of B[*c*]Ph, including **8aNO$_2$**, **8bNO$_2$**, and **8cNO$_2$** with a nitro group in the fjord region. The X-ray structure of **8aNO$_2$** is consistent with severe nitro buttressing.

Experimental Section

General. NMR spectra were recorded at 500 MHz for low-temperature stable ion studies and at 500 MHz or at 400 MHz in room-temperature studies. Electrospray-MS (ES-MS) spectra were obtained by infusion mode by mixing a dilute MeOH solution of the product (10 μM) with AgOTs (30 μM) in MeOH to form PAH/Ag^+ adducts.[12] Because of the existence of two stable isotopes for both silver and bromine atoms, only the averaged *m*/*z* values are reported to simplify the description of the mass spectra. IR spectra were recorded on an FT-IR instrument.

(12) Laali, K. K.; Hupertz, S.; Temu, A. G.; Galembeck, S. E. *Org. Biomol. Chem.* **2005**, *3*, 2319.

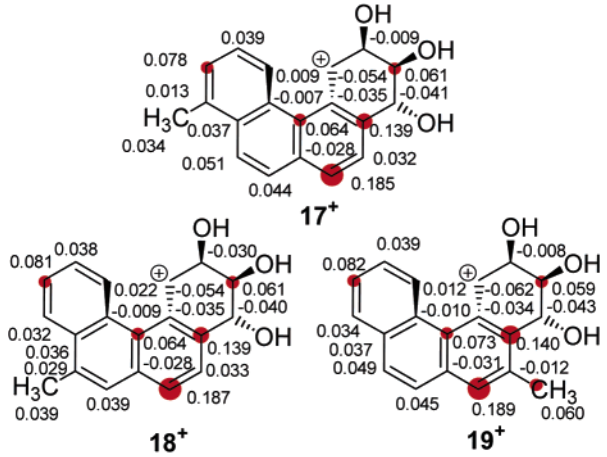

FIGURE 9. NPA-derived changes in charges over CHs relative to neutral precursors (dark circles are roughly proportional to the magnitude of changes; threshold = 0.06).

FSO_3H was distilled twice under argon in an all-glass distillation apparatus at atmospheric pressure and stored under argon at −20 °C in Teflon bottles with Teflon seals. SO_2ClF was prepared according to a modified procedure of Prakash et al.[13]

Typical Procedure for Stable Carbocation Generation. The substrate (10−15 mg) was charged into a 5 mm NMR tube, flushed with argon, and cooled to the dry ice−acetone temperature. SO_2ClF (∼0.3 mL) was condensed directly into the tube. Then, 4−5 drops of FSO_3H were slowly added under argon to prevent local overheating, whereupon an immediate color change took place (variable from compound to compound). After vigorous (vortex) stirring at −78 °C, 3−4 drops of CD_2Cl_2 were slowly introduced into the NMR sample with further vigorous stirring to give a homogeneous solution.

Quenching Procedure. The superacidic solution was carefully poured into a cold aqueous solution of sodium bicarbonate and extracted three times with dichloromethane. The organic extract was dried over magnesium sulfate, filtered, and concentrated under reduced pressure, and the resulting solid residue was assayed by ^{1}H NMR.

X-Ray Crystallographic Data. X-ray crystallography was performed by mounting each crystal onto a thin glass fiber from a pool of Fluorolube and immediately placing it under a liquid N_2 stream, on an X-ray diffractometer. The radiation used was graphite monochromatized Mo Kα radiation (λ = 0.7107 Å). The lattice parameters were optimized from a least-squares calculation on carefully centered reflections. Lattice determination, data collection, structure refinement, scaling, and data reduction were carried out using the APEX2 version 1.0−27 software package. Each structure

(13) Reddy, V. P.; Bellew, D. R.; Prakash, G. K. S. *J. Fluorine Chem.* **1992**, *56*, 195.

(14) Frisch, M. J.; Trucks, G. W.; Schlegel, H. B.; Scuseria, G. E.; Robb, M. A.; Cheeseman, J. R.; Montgomery, J. A., Jr.; Vreven, T.; Kudin, K. N.; Burant, J. C.; Millam, J. M.; Iyengar, S. S.; Tomasi, J.; Barone, V.; Mennucci, B.; Cossi, M.; Scalmani, G.; Rega, N.; Petersson, G. A.; Nakatsuji, H.; Hada, M.; Ehara, M.; Toyota, K.; Fukuda, R.; Hasegawa, J.; Ishida, M.; Nakajima, T.; Honda, Y.; Kitao, O.; Nakai, H.; Klene, M.; Li, X.; Knox, J. E.; Hratchian, H. P.; Cross, J. B.; Bakken, V.; Adamo, C.; Jaramillo, J.; Gomperts, R.; Stratmann, R. E.; Yazyev, O.; Austin, A. J.; Cammi, R.; Pomelli, C.; Ochterski, J. W.; Ayala, P. Y.; Morokuma, K.; Voth, G. A.; Salvador, P.; Dannenberg, J. J.; Zakrzewski, V. G.; Dapprich, S.; Daniels, A. D.; Strain, M. C.; Farkas, O.; Malick, D. K.; Rabuck, A. D.; Raghavachari, K.; Foresman, J. B.; Ortiz, J. V.; Cui, Q.; Baboul, A. G.; Clifford, S.; Cioslowski, J.; Stefanov, B. B.; Liu, G.; Liashenko, A.; Piskorz, P.; Komaromi, I.; Martin, R. L.; Fox, D. J.; Keith, T.; Al-Laham, M. A.; Peng, C. Y.; Nanayakkara, A.; Challacombe, M.; Gill, P. M. W.; Johnson, B.; Chen, W.; Wong, M. W.; Gonzalez, C.; Pople, J. A. *Gaussian 03*, revision C.02; Gaussian, Inc.: Wallingford, CT, 2004.

SCHEME 4. Nitration/Bromination Reactions of Compounds 2, 4, and 5

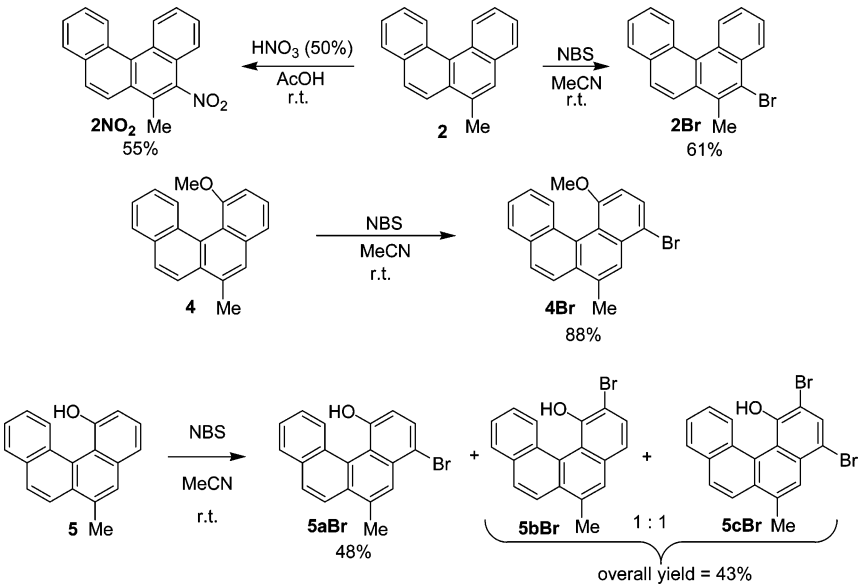

SCHEME 5. Nitration/Bromination Reactions of Compounds 8, 9, and 11

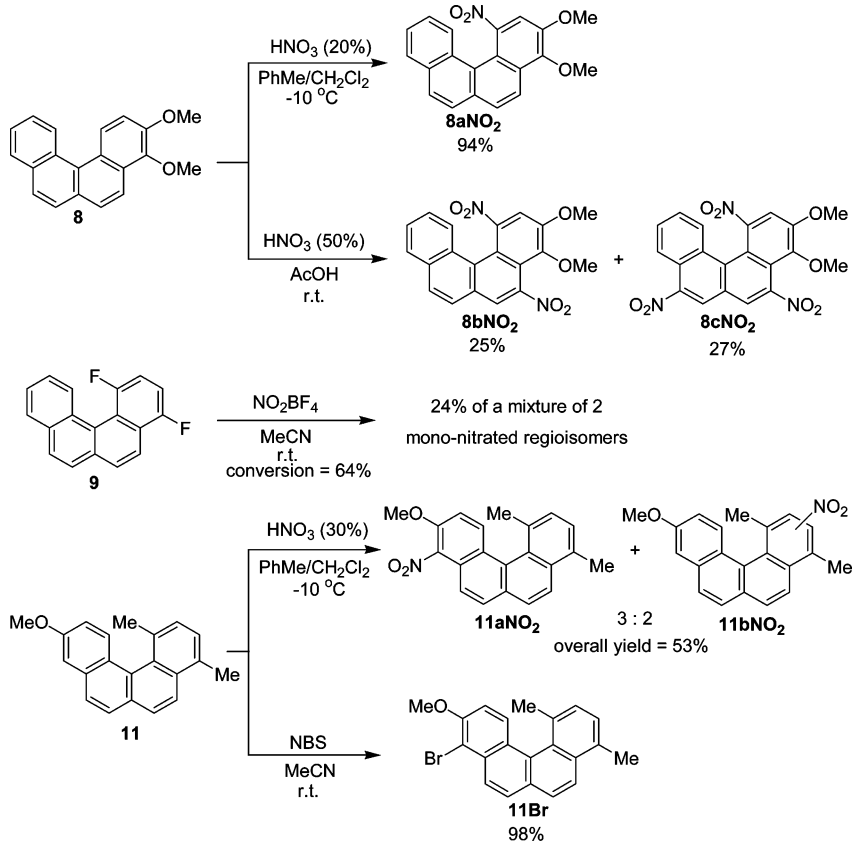

was solved using direct methods. This procedure yielded a number of the C, N, and O atoms. Subsequent Fourier synthesis yielded the remaining atom positions. The hydrogen atoms were fixed in positions of ideal geometry and refined within the XSHELL software. These idealized hydrogen atoms had their isotropic temperature factors fixed at 1.2 or 1.5 times the equivalent isotropic U of the C atoms to which they were bonded. The final refinement of each compound included anisotropic thermal parameters on all non-hydrogen atoms.

Computational Protocols. Structures were optimized using a C_1 molecular point group, except for B[*c*]Ph (C_2), by the density function theory (DFT) method at the B3LYP/6-31G(d) level using the Gaussian 03 package.[14] All computed geometries were verified by frequency calculations to have no imaginary frequencies. Energies of the optimized structures for benzo[*c*]phenanthrene (**1**), 2-hydroxybenzo[*c*]phenanthrene, and their protonation cations are summarized in Table S1 in the Supporting Information. NMR chemical shifts were calculated by the GIAO[15] method at the B3LYP/6-31G(d) level. NMR chemical shifts were referenced to

(15) Wolinski, K.; Hinton, J. F.; Pulay, P. *J. Am. Chem. Soc.* **1990**, *112*, 8251. Ditchfield, R. *Mol. Phys.* **1974**, *27*, 789.

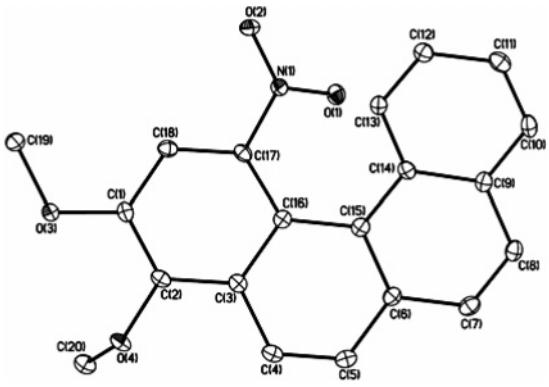

FIGURE 10. Thermal ellipsoid plot of **8aNO$_2$** (ellipsoids are drawn at the 30% level).

TMS (GIAO magnetic shielding tensor = 189.8 ppm in TMS; these values are related to the GIAO isotropic magnetic susceptibility for ^{13}C), calculated with the molecular symmetry of T_d at the same level of theory (Figure 6). Natural population analysis (NPA)-derived charges were computed at the same level (Figures 7 and 8).

Global minima for 2-hydroxy-B[*c*]Ph and 2-hydroxy-2-benzo-[*c*]phenanthrenium ions were located by changing the direction of the O−H groups and the H−C−O geometry and by comparing the resulting optimized structures and their energies. Changes in the NPA-derived charges relative to the corresponding neutrals were found to be very close (almost the same) among the isomers. Therefore, only representative conformational isomers for the diol epoxides and their corresponding ring-opened carbocations were computed to derive charge delocalization modes via changes in the NPA-derived charges.

Acknowledgment. We thank Dr. Scott Bunge (KSU) for the X-ray analysis. Support of this study under "reactive intermediates of carcinogenesis of PAHs" by the NCI of the NIH (2R15-CA078235-02A1) is gratefully acknowledged. M.K.L. acknowledges support via Grant S06 GM008168-24S1 (NIGMS) and infrastructural support at CCNY via NIH RCMI Grant 5G 12 RR03060-20.

Supporting Information Available: Experimental method, compound characterization, and energies and Cartesian coordinates for the optimized structures (for selected carbocations) by B3LYP/6-31G(d) (Tables S1−S6). Crystallographic information file (CIF) for compound **8aNO$_2$**. This material is available free of charge via the Internet at http://pubs.acs.org.

JO0625453